Interrelation between Substrate Roughness and Thin-Film Structure of Functionalized Acenes on Graphite

ARTICLE *in* CRYSTAL GROWTH & DESIGN · SEPTEMBER 2011

Impact Factor: 4.89 · DOI: 10.1021/cg200894y

CRYSTAL GROWTH & DESIGN

ARTICLE

pubs.acs.org/crystal

Interrelation between Substrate Roughness and Thin-Film Structure of Functionalized Acenes on Graphite

Tobias Breuer,[†] Ingo Salzmann,[‡] Jan Götzen,[†] Martin Oehzelt,[‡] Antonia Morherr,[†] Norbert Koch,[‡] and Gregor Witte*[,†]

[†]Molekulare Festkörperphysik, Philipps-Universität Marburg, D-35032 Marburg, Germany

[‡]Institut für Physik, Humboldt-Universität zu Berlin, D-12489 Berlin, Germany

Supporting Information

ABSTRACT: Using atomic force microscopy (AFM) and X-ray diffraction (XRD), we analyzed the growth of differently modified pentacenes (perfluoropentacene and pentacenetetrone) on graphite and demonstrate that both the resulting morphology and the crystalline structure of the films critically depend on the microroughness of the substrate. On well-ordered highly oriented pyrolytic graphite (HOPG) surfaces prepared by exfoliation, both molecular materials form exceptionally smooth films, which consist of large-area molecularly flat islands yielding an overall low roughness. Interestingly, in these films molecules adopt a recumbent orientation, while on defective substrates, created by brief ion sputtering, the molecules adopt an upright orientation and form nonconnected islands exhibiting a significantly increased film roughness. Our study not only underlines the possibility to prepare very smooth films on a weakly interacting substrate but also emphasizes the importance of a proper substrate preparation and the significance of precise knowledge of substrate-surface properties to control the resulting structure of organic films.

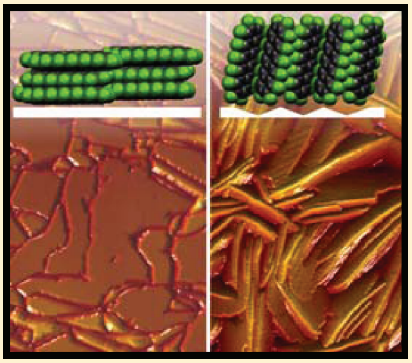

1. INTRODUCTION

Owing to the anisotropic shape of π-conjugated aromatic molecules and the related anisotropic intermolecular interactions, these compounds generally adopt complex packing motifs in the crystalline phase, like, for example, layered stacking and/or herringbone arrangements.[1] These structural features also result in a pronounced anisotropy of electronic and optical properties of organic crystals[2] and crystalline molecular films.[3−6] Therefore, precise control of molecular and crystalline orientation during film growth is inevitable to utilize and explore the remarkable optoelectronic properties of such materials. Moreover, it is also of prime importance for an optimized fabrication of organic thin-film devices. Previous studies have shown that the structure of organic films is mainly governed by a competition between intermolecular and molecule−substrate interactions. On metal substrates, this initially favors a recumbent adsorption geometry of planar π-conjugated molecules, whereas an upright orientation is frequently observed on weakly interacting substrates such as SiO_2.[7] Subsequent molecular film growth on metals is in many cases accompanied by distinct dewetting and island formation,[8−10] while the actual molecular orientation depends critically on the surface roughness. In contrast to molecular films that were grown on well-ordered single-crystalline metal surfaces, the recumbent molecular orientation of the lowermost seed-layer is not retained in multilayer films if grown on polycrystalline metals. There, a preferential upright molecular orientation has been observed for various molecular compounds including diindenoperlyene, phthalocyanines, and pentacene.[11−14] A similar situation was also reported upon growth of sexithiophene films on $TiO_2(110)$, which exhibit distinct needles with recumbent molecular orientation mediated by the substrate, while on poorly ordered surfaces islands with upright-oriented molecules are formed.[15]

Previously, we have shown that particularly smooth pentacene films can be grown on graphite exhibiting molecularly flat islands, which extend over several micrometers.[16] Despite a rather weak molecule−graphite interaction,[17] the molecules adopt a recumbent orientation in such films, which is caused by a prealignment in the initial stage of film growth due to a perfect match between the molecular carbon frame and the surface lattice of the graphite basal plane.[16] Moreover, it could be demonstrated that the weak substrate interaction allows a small molecular reorientation in the lowermost layer and thus a relief of strain caused by the structural misfit between the molecular arrangement in the physisorbed wetting layer and the crystalline bulk phase. Finally, it was found that this particular growth mode depends sensitively on the surface quality since a quite different growth scenario occurs on defective surface regions where pentacene forms islands with upright molecular orientation.

Here, we report a comparative growth study of the two chemically modified pentacene derivatives perfluoropentacene (PFP) and 5,7,12,14-pentacenetetrone (PTET). Though both molecules are planar, they exhibit dissimilar crystal structures,[18,19] which is related

Received: July 14, 2011
Revised: September 6, 2011
Published: September 15, 2011

to distinct differences in the intramolecular charge distributions. This poses the question about the general ability of graphite to control the molecular orientation in adsorbed thin films. Combining atomic force microscopy (AFM) and X-ray diffraction (XRD) measurements, we demonstrate that, indeed, long-range ordered and exceedingly smooth films with recumbent molecular orientation can be prepared also for such functionalized acenes and that the resulting film structure depends critically on the roughness of the substrate surface. While PTET exhibits the known crystalline bulk phase,[19] PFP films adopt a new polymorph, which had been found previously also for PFP films that were deposited onto Ag(111) surfaces.[20] In contrast to this finding for pristine exfoliated highly oriented pyrolytic graphite (HOPG), on microscopically rough graphite substrates prepared by brief sputtering both materials grow in their respective bulk phases and exhibit upright molecular orientations.

2. EXPERIMENTAL SECTION

All molecular films were grown onto ZYA-grade highly oriented pyrolytic graphite (HOPG) substrates (SPI supplies, mosaicity < 0.4°), which, in each case, were prepared by exfoliation in air before loading into the ultra-high vacuum (UHV) chamber. Particular care was taken to avoid graphite flakes sticking out of the sample, which easily can adhere to the AFM tip by sleeking the cleaved surfaces. The graphite substrates were mounted onto sample holders either by conductive adhesion tape (Plano) or by metal clips, which also enable sample heating prior to deposition. To investigate the influence of surface roughness on the molecular film growth, some of the cleaved HOPG substrates were intentionally modified by Ar^+-sputtering ($E = 700$ eV, $I = 5\ \mu$A), and the resulting surface ordering was monitored by low energy electron diffraction (LEED).

PFP (Kanto Denka Kogoyo Co. LTD) and PTET (Avocado Organics) films were deposited under high vacuum conditions (base pressure < 5×10^{-9} mbar) by organic molecular beam deposition from alumina crucibles of a resistively heated Knudsen cell at deposition rates of 6 Å/min monitored by quartz crystal microbalance.

The morphology of the various films was characterized at ambient conditions by means of atomic force microscopy (AFM, Agilent SPM 5500) operated in tapping mode at cantilever frequencies of about 300 kHz. The XRD measurements were carried out under He atmosphere at the W1 beamline at DESY-HASYLAB (Hamburg). Optical microscopy in combination with a linear polarizer was employed to obtain complementary information about the lateral size of the crystallites within the films.

3. RESULTS

3.1. PFP and PTET Films on Pristine Graphite. Figure 1 compares the morphology and crystalline orientation of PFP and PTET films with a nominal thickness of 50 nm that were deposited at room temperature onto freshly cleaved HOPG substrates. AFM data show that films of both materials consist of compact and densely packed mesa-like islands extending over several micrometers that are separated by deep and narrow trenches. High resolution AFM images yield a roughness of less than 0.2 nm for the individual island surfaces (cf. magnified line scans in Figure 1b,f), thus indicating that the islands appear to be molecularly flat. Only in the case of PTET some islands reveal characteristic depressions with a depth of about 20 nm on the otherwise flat islands (indicated by black arrows in the inset of Figure 1e). A quantitative analysis yields highly uniform island heights, thus demonstrating overall very smooth organic films. This is remarkable since previous studies have revealed a substantial roughness for PFP films grown onto SiO_2 or Ag(111) substrates.[21,10]

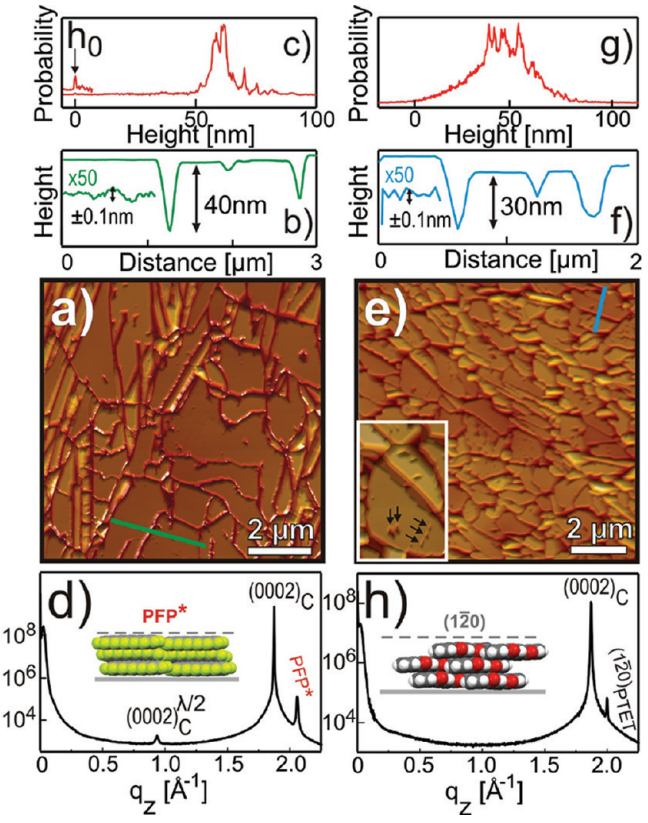

Figure 1. Comparison of PFP (lhs) and PTET films (rhs) of nominal thickness of 50 nm grown at room temperature onto freshly cleaved HOPG substrates: (a, e) AFM micrographs together with corresponding line scans and height distributions (b, c, f, g). Corresponding specular XRD-data are shown in panels (d, h) and the resulting molecular arrangements are sketched in the respective insets.

Using specular X-ray diffraction, the crystalline orientation of the molecular films was identified. Typical XRD results are depicted in Figure 1d,h and exhibit a dominating substrate related C(0002) diffraction peak at $q_z = 1.87$ Å^{-1} (corresponding to an interlayer spacing of the graphite basal planes of 3.36 Å). For the PTET film, an additional diffraction peak appears at $q_z = 2.00$ Å^{-1} (cf. Figure 1h). With a corresponding lattice plane distance of 3.142 Å, this peak can be unambiguously identified as (1 $\bar{2}$ 0) peak of the PTET bulk structure,[19] thus reflecting a recumbent molecular orientation in such films as sketched in the inset of Figure 1h.

In addition to the C(0002) substrate reflection, the diffractogram of the PFP film (shown in Figure 1d) reveals two further peaks at $q_z = 0.937$ Å^{-1} and $q_z = 2.06$ Å^{-1}. While the first is assigned to the $\lambda/2$ contribution of the substrate reflection, which is visible here due to a significantly larger thickness of the HOPG crystal used in this experiment, the peak at higher momentum transfer is assigned to PFP. It corresponds to a lattice spacing of 3.05 Å, which does not match any reflection of the PFP bulk structure[18] or the PFP thin-film phase,[22] which therefore demonstrates the presence of a new surface-mediated PFP polymorph that was already reported for Ag(111) substrates.[20] Note that there a PFP herringbone structure of (inclined) lying molecules could be deduced from XRD and photoemission data for this specific polymorph.

Though AFM data reveal the presence of very smooth islands, their lateral crystalline ordering, especially the size of single-crystalline

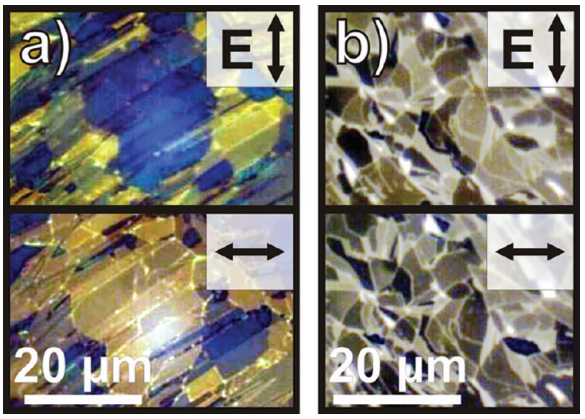

Figure 2. Polarization microscopy micrographs of (a) PFP and (b) PTET films with a nominal thickness of 50 nm grown at 325 K on pristine HOPG substrates that were recorded with linearly polarized light at different orientations as indicated by the black arrow.

regions, cannot be concluded directly because rotational domains within the islands are still possible. Similarly, the XRD Θ/2Θ scans clearly prove the crystallinity of the films but cannot judge the lateral single-crystallinity of the individual islands. Since the various optical excitations of aromatic molecules like PFP have differently oriented transition dipole moments,[6] the color appearance of the islands observed by polarization microscopy can be used to obtain complementary information about the domain size. Figure 2 displays a series of optical micrographs of PFP and PTET films taken for linear polarized light with different angles of polarization. In order to increase the size of individual islands, the films had actually been deposited at a slightly higher substrate temperature of 325 K, which yields island diameters of more than 10 μm. While the islands appear azimuthally distributed due to the polycrystallinity of the HOPG substrate, they exhibit a rather homogeneous polarization contrast within the individual islands, thus reflecting their homogeneous crystalline structure.

3.2. PFP and PTET Film Growth on Defective Graphite Surfaces. In a previous study, it was reported that the resulting morphology and crystalline orientation of pentacene films grown on HOPG depend sensitively on the actual surface roughness.[16] Therefore, we have also investigated the structure of PFP and PTET films grown onto graphite substrates, which had been intentionally roughened by sputtering. To analyze the influence of such a treatment, first of all the quality of the graphite surface and its degradation upon sputtering were characterized by means of AFM and LEED. Figure 3a,b compares two AFM micrographs that were taken at the same position of a HOPG substrate before and after Ar^+-ion sputtering (5 min, 700 eV). An inspection of these images shows that the morphology does not change dramatically. The general morphology remains unchanged, while a significant increase of surface roughness occurs. Please note that the depicted image must not be misinterpreted as a real image of atomic defects, as the resolution of the AFM is too low to resolve those defects directly. However, the increased roughness (rms of the sputtered substrate 0.17 nm compared to 0.061 nm of the defect-free surface) is a clear indication of degrading substrate quality. This finding is supported as a rapid degradation of the substrate LEED pattern with sputtering time was observed. The LEED pattern of the pristine HOPG surface prepared by exfoliation reveals a characteristic ring pattern, which reflects its

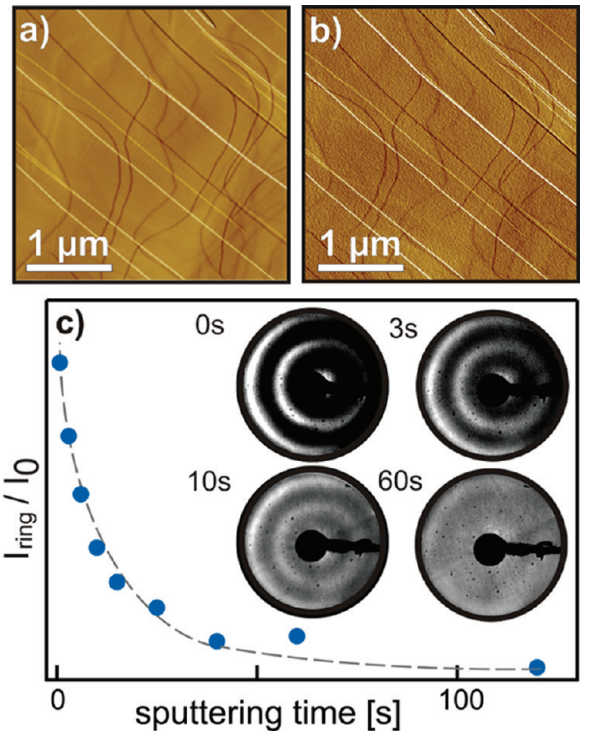

Figure 3. Surface degradation of an exfoliated HOPG surface upon subsequent Ar^+-ion sputtering (700 eV). AFM micrographs recorded (a) before and (b) after 2 min of sputtering reveals enhanced substrate roughness; electron diffraction (c) reveals a rapid disappearance of the substrate LEED pattern (E = 180 eV) as a function of the sputtering time.

high local ordering but azimuthal isotropy of the graphite flakes within the surface. Figure 3c depicts the diffraction ring to background intensity ratio, which becomes halved already after bombardment times of only 6 s, while after 2 min the ring pattern was no longer visible thus indicating severe damaging of the surface lattice. From this characterization, we conclude that room temperature sputtering essentially creates point defects, which destroy the coherence of the graphite surface lattice but does not increase the step density.

Figure 4 compares the resulting morphology and crystalline orientation of PFP and PTET films that were grown on HOPG substrates, which had been sputtered for 5 min prior to deposition. Rather different film structures are observed, which is strikingly illustrated by the AFM data recorded for a 50 nm PFP film depicted in Figure 4a−c. Instead of a smooth layer, the film consists of elongated spicular islands with a length of several micrometers and a width of 100−300 nm, that are laterally isotropically distributed along the sample yielding an overall large roughness of more than 20 nm. This morphology parallels the situation observed before for PFP films grown onto SiO_2.[21] Like in that case, characteristic steps of about 1.5 nm were identified (cf. line scan Figure 4b), which is in close agreement with the interlayer distance of (100)-planes, hence indicating an upright molecular orientation. To verify if this locally observed orientation is characteristic for the entire sample, XRD measurements were carried out for this sample. The corresponding XRD scan that is shown in Figure 4d reveals beside the (0002) diffraction peak of the substrate (at $q_z = 1.873$ Å^{-1}) three PFP-related peaks at $q_z = 0.401$ Å^{-1}, $q_z = 0.805$ Å^{-1}, and $q_z = 1.208$ Å^{-1}. These peak positions are in excellent agreement with the (n00)-reflexes of

dx.doi.org/10.1021/cg200894y |*Cryst. Growth Des.* 2011, 11, 4996–5001

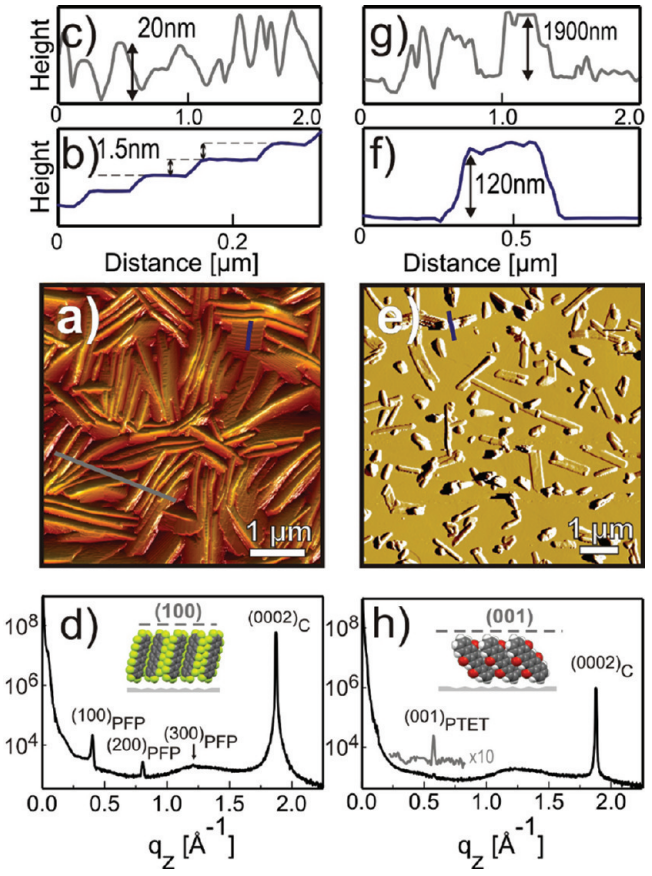

Figure 4. Morphology and crystalline structure of PFP (lhs) and PTET films (rhs) grown on HOPG substrates that were intentionally roughened by brief Ar^+ sputtering (5 min): (a) AFM micrograph of a 50 nm PFP film with (b, c) corresponding line scans, and (e) AFM micrograph (amplitude image) of a nominal 3 nm PTET film with (f) corresponding topographical line scan while (g) reveals a line scan of a 50 nm PTET film, which could not be imaged properly. Accompanying specular XRD scans are shown in panels (d) for a 50 nm PFP film and (h) for a 50 nm PTET film. The molecular orientations in the films are sketched in the insets.

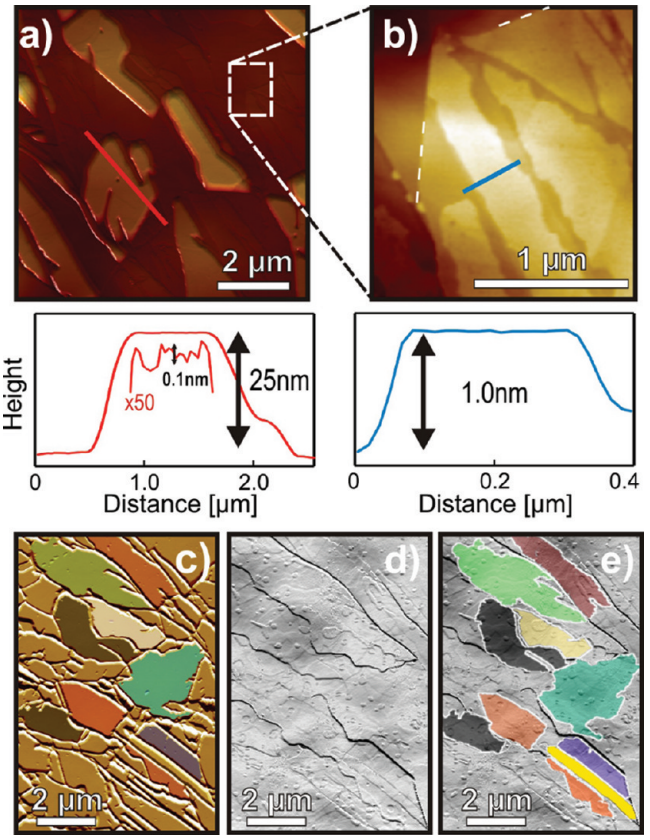

Figure 5. AFM micrograph showing the morphology of 5 nm PFP deposited (a) on pristine HOPG together with (b) magnified image and corresponding line scans. Panels (c−e) show a comparison of a 40 nm PFP film deposited on pristine HOPG and (d) the bare surface after thermal desorption of the film. In panel (e) tagged islands from (c) are superimposed onto the bare surface.

the PFP-thin film phase[22] ($q_{z,(100)}$ = 0.399 Å^{-1}, $q_{z,(200)}$ = 0.797 Å^{-1}, $q_{z,(300)}$ = 1.196 Å^{-1}), thus proving an overall upright orientation of PFP molecules on the sputtered HOPG substrate.

Supporting XRD reciprocal space mapping experiments of this film confirmed that on the rough substrate molecules actually crystallize only in this polymorph — instead of the PFP single-crystal phase[18] or the new polymorph observed for the case of pristine HOPG (data shown in Supporting Information).

Likewise, a strikingly different morphology was also observed for PTET films that were deposited onto sputtered HOPG substrates. In that case a pronounced dewetting takes place and leads to the formation of extremely elevated islands exceeding even a height of 2 μm at a nominal film thickness of 50 nm (cf. line scan Figure 4g), which, however, impeded the acquisition of satisfying AFM images. Therefore, the morphology of much thinner films was characterized. Figure 4e shows such a typical amplitude AFM image of a PTET film with a nominal thickness of 3 nm, which reveals the presence of elongated mesa-shaped islands with heights of more than 100 nm at widths of about 200 nm. Though the mentioned roughness obviated precise AFM imaging for a 50 nm thick film, XRD scans are, by nature, not affected by this limitation. The corresponding XRD scan (see Figure 4h) reveals in addition to the C(0002) substrate peak a weak but distinct diffraction peak at q_z = 0.576 Å^{-1}. The corresponding lattice spacing of d = 10.91 Å is in good agreement with the (001) lattice spacing of the PTET bulk phase. In this texture, the molecules are rather upright-oriented and their long axis adopts an angle of about 42° with respect to the sample surface, as shown schematically in the inset in Figure 4h.

3.3. Initial Stage of Film Growth. To fathom the influence of the substrate surface structure on molecular film growth and possible limitations of the island sizes additional AFM measurements were carried out for the initial stage of PFP deposition. Figure 5a shows an AFM micrograph of a PFP film with a nominal thickness of 5 nm deposited onto a pristine HOPG substrate. At this initial growth stage rather large mesa-shaped islands with a height of more than 20 nm are formed that reveal molecularly flat surfaces extending over several micrometers. In addition, they are surrounded by distinctly lower and less extended islands exhibiting a height of only 1 nm corresponding to just a few monolayers as shown by the magnified micrograph in Figure 5b. Comparing the shape of such lower islands and the position of substrate steps (cf. dashed line in Figure 5b) suggests that the size of the molecular islands is limited by steps and/or grains of the substrate. To further study this effect AFM was employed to compare the island shape occurring in a 40 nm PFP film with the corresponding morphology of the underlying HOPG

dx.doi.org/10.1021/cg200894y |*Cryst. Growth Des.* 2011, 11, 4996–5001

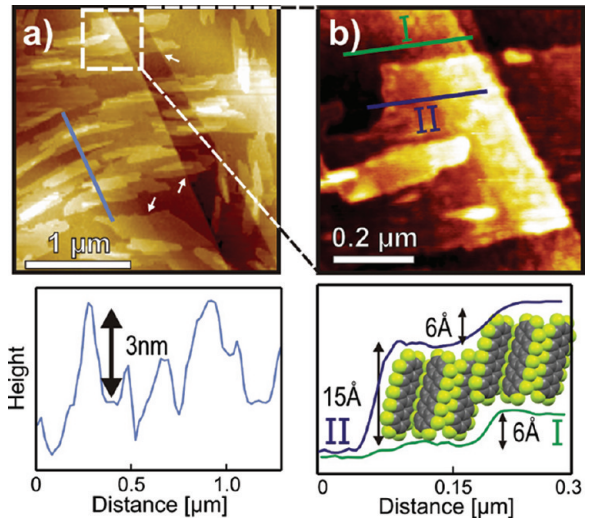

Figure 6. AFM micrographs showing the initial stage of PFP film formation on a sputtered HOPG substrate together with corresponding line scans. The magnified image b) reveals the appearance of a dislocation within the PFP film induced by an underlying substrate double-step.

substrate. For this purpose the PFP film was thermally desorbed in a vacuum chamber by heating the sample at 450 K for 10 min. Figure 5c−e shows the result of this experiment. One can easily verify that the images show the same area of the sample, as characteristic edges can be identified in both cases. Note that the visible edges represent different grain-boundaries. While they reveal a topographic contrast of PFP island-borders within the film (Figure 5c) they represent substrate edges of the bare surface, which are enhanced in the AFM amplitude image shown in Figure 5d. By superimposing the contour of individual islands, which are color tagged in Figure 5c onto the bare HOPG surface of the same position this effect becomes even more explicit (cp. Figure 5d,e). This analysis proves that the island sizes are actually limited by the density of step edges and the grain size of the substrate.

Finally, we investigated the initial growth of PFP films on sputtered HOPG surfaces. In contrast to the growth scenario on pristine HOPG the molecules nucleate in rather small, azimuthally isotropically distributed spicular islands as shown in Figure 6 for a PFP film with a nominal thickness of about 4 nm. The high nucleation density of these islands leads to a rather high coverage of the substrate surface, while thicker films (cf. Figure 4a) exhibit a substantial roughness. The observed islands again show characteristic molecular steps of 1.5 nm, which reflect the upright molecular orientation. Since again substrate steps are clearly observed, their influence on the island growth can be followed. The overview image depicted in Figure 6a exhibits many spicular islands that extend over such substrate steps (indicated by white arrows). A closer inspection (see magnified image in Figure 6b) further reveals that upright-oriented molecules are capable of overgrowing small substrate steps by creating dislocations within the molecular adlayer as illustrated by the corresponding line scans.

4. DISCUSSION

In the present study, we have analyzed the film formation of the pentacene derivatives perfluoropentacene and pentacenetetrone on HOPG substrates with particular emphasis on the influence of substrate roughness.

Previous studies have already shown that organic electronic device properties depend critically on the substrate roughness.[23,24] For instance, the grain size within organic films is affected by the quality of the dielectric surfaces and their actual chemical termination.[25] However, detailed microscopic investigations were hampered by the amorphous nature of the substrates used.

The present data demonstrate that film growth on graphite substrates of different surface quality (pristine vs sputtered) does not only result in very unequal film roughnesses but that the films also exhibit entirely different molecular and crystalline orientations. On microscopically rough HOPG surfaces, the studied molecules grow in an upright orientation and form crystalline islands exhibiting their respective bulk phase. In contrast, on pristine HOPG substrates films of recumbently oriented molecules are formed and, in case of PFP, even exhibit growth in a different polymorph. These findings are in good concordance with a former study regarding the growth of pentacene on HOPG,[16] suggesting that the observed effect is general for different acenes and not only a peculiarity of pentacene. Different molecular orientations have also been reported for acenes grown on metals of different roughness, for example, for pentacene on single and polycrystalline gold.[13] Interestingly, however, the film roughness appears to be inverted: While on single crystalline metal substrates highly ordered wetting layers are formed, which are stabilized by electronic interaction (chemisorption), the subsequent layers exhibit substantial islanding and are significantly rough. We note that the actual molecular orientation in such films can be rather different since in some cases upright-oriented molecules are found while they remain recumbently oriented in other cases.[9,13,26−28]

Most notably, although any additional chemical substrate interactions of pentacene and its derivatives can be excluded on graphite substrates, they form remarkably smooth films on pristine surfaces. We attribute this exceptional film growth to the good match of the carbon frame of the acenes with the lattice of the basal plane of graphite: A comparison between the ring diameters of PFP (2.77 Å), PTET (2.78 Å (H-terminated), 2.80 Å (O-terminated)), PEN (2.81 Å), and graphite (2.85 Å) shows a close match, which suggests a template effect by the formation of a commensurate seed layer on the HOPG surface. Moreover, as demonstrated previously for the case of pentacene on HOPG,[16] the low adsorption energy additionally allows a slight rearrangement of the adsorbed molecules, thus enabling adjustment to the packing motif of the crystalline structure. Apparently, this prealignment causes PFP molecules to grow in recumbent orientation and to form a new polymorph. While this polymorph is observed also for PFP films grown on Ag(111),[20] there, in clear contrast, the films exhibit a substantial roughness.[10] A comparison of the shape of PFP islands on pristine HOPG and the morphology of the underlying substrate shows that the island size is actually limited by the size of substrate grains, hence indicating that such grain boundaries are efficient diffusion barriers during growth. Note that such a specific nucleation and grain-limited growth was also observed before for the growth of *p*-quaterphenylene films on polycrystalline gold.[29−31]

A completely different situation occurs on sputtered HOPG substrates. Because of the lack of any templating effect, which would cause a prealignment upon nucleation, and because of a larger nucleation density on the rough surface, the film growth most likely is goverened by a minimization of surface energy. Like in the case of chemically inert substrates, for example, SiO_2, this leads to upright-oriented molecules forming fiber-textures with (100)-oriented surfaces, where molecules adopt a high coordination and, thus, a low surface energy.

On the basis of AFM data of the initial stage of growth, it was found that upright-oriented PFP molecules are able to overgrow low defect steps of the substrate by creating dislocations within the film (cf. Figure 6b). Interestingly, this ability was not observed for PTET and is attributed to the oxygen side groups whose repulsive interaction requires interdigitation, thus allowing only for specific lateral shifts of neighboring molecules.

5. CONCLUSION

The present growth study of acene derivatives on HOPG substrates of different surface quality (roughness) demonstrates that the resulting crystalline structure of such molecular films is not only controlled by the interplay of molecule−substrate and molecule−molecule interactions but also depends sensitively on the single-crystalline coherence length of the substrate. Pristine HOPG substrates with a low defect density are demonstrated to be well-suited templates for preparing particularly smooth acene films consisting of largely extended and molecularly flat islands. In such films, pentacene as well as pentacenetetrone and perfluoropentacene adopt a recumbent orientation, which, in case of PFP, is enabled by a new polymorph. The remarkable order in these films makes them interesting model systems for further optical and electronic studies to characterize the influence of packing motifs on the opto-electronic properties of such functional molecular materials.

■ ASSOCIATED CONTENT

Supporting Information. Supporting X-ray diffraction reciprocal space mapping data of a PFP thin film deposited on a sputtered HOPG substrate. This information is available free of charge via the Internet at http://pubs.acs.org/.

■ AUTHOR INFORMATION

Corresponding Author

*E-mail: gregor.witte@physik.uni-marburg.de.

■ ACKNOWLEDGMENT

We thank Wolfgang Caliebe (DESY - HASYLAB) for experimental support and A. Moser (TU-Graz, Austria) for providing computational support for RSM data analysis. T.B. acknowledges financial support by the Friedrich-Ebert-Stiftung. M.O. acknowledges financial support by the Austrian Science Fund (FWF) project P21094−N20.

■ REFERENCES

(1) Anthony, J. E. *Chem. Rev.* **2006**, *106*, 5028.
(2) Karl, N., Farchioni, R., Grosso, G., Eds. *Organic Electronic Materials*; Springer: New York, 2001.
(3) Duhm, S.; Heimel, G.; Salzmann, I.; Glowatzki, H.; Johnson, R. L.; Vollmer, A.; Rabe, J. P.; Koch, N. *Nat. Mater.* **2008**, *7*, 326.
(4) Ueno, N.; Kera, S. *Prog. Surf. Sci.* **2008**, *83*, 490.
(5) Sassella, A.; Borghesi, A.; Meinardi, F.; Tubino, R.; Gurioli, M.; Botta, C.; Porzio, W.; Barbarella, G. *Phys. Rev. B* **2000**, *62*, 11170.
(6) Breuer, T.; Witte, G. *Phys. Rev. B* **2011**, *83*, 155428.
(7) Witte, G.; Wöll, Ch. *J. Mater. Res.* **2004**, *19*, 7.
(8) Stöhr, M.; Gabriel, M.; Möller, R. *Europhys. Lett.* **2002**, *59*, 423.
(9) Käfer, D.; Witte, G. *Chem. Phys. Lett.* **2007**, *442*, 376.
(10) Götzen, J.; Schwalb, C. H.; Schmidt, C.; Mette, G.; Marks, M.; Höfer, U.; Witte, G. *Langmuir* **2001**, *27*, 993.
(11) Dürr, A. C.; Koch, N.; Kelch, M.; Ghijsen, J.; Johnson, R. L.; Pireaux, J. J.; Schwartz, J.; Schreiber, F.; Dosch, H.; Kahn, A. *Phys. Rev. B* **2003**, *68*, 115428.
(12) Peisert, H.; Biswas, I.; Zhang, L.; Knupfer, M.; Hanack, M.; Dini, D.; Batchelor, D.; Chasse, T. *Surf. Sci.* **2006**, *600*, 4024.
(13) Käfer, D.; Ruppel, L.; Witte, G. *Phys. Rev. B* **2007**, *75*, 085309.
(14) Zheng, Y.; Wee, A. T. S.; Chandrasekhar, N. *ACS Nano* **2010**, *4*, 2104.
(15) Ivanco, J.; Haber, T.; Krenn, J. R.; Netzer, F. P.; Resel, R.; Ramsey, M. G. *Surf. Sci.* **2007**, *601*, 178.
(16) Götzen, J.; Käfer, D.; Wöll, Ch.; Witte, G. *Phys. Rev. B* **2010**, *81*, 085440.
(17) Zacharia, R.; Ulbricht, H.; Hertel, T. *Phys. Rev. B* **2004**, *69*, 155406.
(18) Sakamoto, Y.; Suzuki, T.; Kobayashi, M.; Gao, Y.; Fukai, Y.; Inoue, Y.; Sato, F.; Tokito, S. *J. Am. Chem. Soc.* **2004**, *126*, 8138.
(19) Käfer, D.; El Helou, M.; Gemel, Ch.; Witte, G. *Cryst. Growth Des.* **2008**, *8*, 3053.
(20) Duhm, S.; Hosoumi, S.; Salzmann, I.; Gerlach, A.; Oehzelt, M.; Wedl, B.; Lee, T. L.; Schreiber, F.; Koch, N.; Ueno, N. *Phys. Rev. B* **2010**, *81*, 045418.
(21) Kowarik, S.; Gerlach, A.; Hinderhofer, A.; Milita, S.; Borgatti, F.; Zontone, F.; Suzuki, T.; Biscarini, F.; Schreiber, F. *Phys. Status Solidi (RRL)* **2008**, *2*, 120.
(22) Salzmann, I.; Duhm, S.; Heimel, G.; Rabe, J. P.; Koch, N.; Oehzelt, M.; Sakamoto, Y.; Suzuki, T. *Langmuir* **2008**, *24* (14), 7294.
(23) Jung, Y.; Kline, R. J.; Fischer, D. A.; Liu, E. K.; Heeny, M.; McCulloch, I.; DeLongchamp, D. M. *Adv. Funct. Mater.* **2008**, *18*, 742.
(24) Yang, H.; Yang, C.; Kim, S. H.; Jang, M.; Park, C. E. *ACS Appl. Mater. Interfaces* **2010**, *2*, 391.
(25) Ruiz, R.; Choudhary, D.; Nickel, B.; Toccoli, T.; Chang, K.-C.; Mayer, A. C.; Clancy, P.; Blakely, J. M.; Headrick, R. L.; Iannotta, S.; Malliaras, G. G. *Chem. Mater.* **2004**, *16*, 4497.
(26) Söhnchen, S.; Lukas, S.; Witte, G. *J. Chem. Phys.* **2004**, *121*, 525.
(27) Götzen, J.; Lukas, S.; Birkner, A.; Witte, G. *Surf. Sci.* **2011**, *605*, 577.
(28) Djuric, T.; Ules, T.; Flesch, H. G.; Planck, H.; Shen, Q.; Teichert, C.; Resel, R.; Ramsey, M. G. *Cryst. Growth Des.* **2011**, *11*, 1015.
(29) Müllegger, S.; Mitsche, S.; Pölt, P.; Hänel, K.; Birkner, A.; Wöll, Ch.; Winkler, A. *Thin Solid Films* **2005**, *484*, 408.
(30) Müllegger, S.; Salzmann, I.; Resel, R.; Winkler, A. *Appl. Phys. Lett.* **2003**, *83* (22), 4536.
(31) Müllegger, S.; Salzmann, I.; Resel, R.; Hlawacek, G.; Teichert, C.; Winkler, A. *J. Chem. Phys.* **2004**, *121*, 2272.